Michigan Technological University

Digital Commons @ Michigan Tech

Department of Geological and Mining
Engineering and Sciences Publications

Department of Geological and Mining
Engineering and Sciences

2-15-1999

Comparison of TOMS and AVHRR volcanic ash retrievals from the August 1992 eruption of Mt. Spurr

N. A. Krotkov
Raytheon ITSS Co

O. Torres
Univ. of MD

C. Seftor
Raytheon ITSS Co

A. J. Krueger
Goddard Space Flight Center

A. Kostinski
Goddard Space Flight Center

See next page for additional authors

Follow this and additional works at: https://digitalcommons.mtu.edu/geo-fp

Part of the Geology Commons, Mining Engineering Commons, and the Other Engineering Commons

Recommended Citation

Krotkov, N. A., Torres, O., Seftor, C., Krueger, A. J., Kostinski, A., Rose, W. I., Bluth, G. J., Schneider, D., & Schaefer, S. J. (1999). Comparison of TOMS and AVHRR volcanic ash retrievals from the August 1992 eruption of Mt. Spurr. *Geophysical Research Letters, 26*(4), 455-458. http://dx.doi.org/10.1029/1998GL900278
Retrieved from: https://digitalcommons.mtu.edu/geo-fp/84

Follow this and additional works at: https://digitalcommons.mtu.edu/geo-fp

Part of the Geology Commons, Mining Engineering Commons, and the Other Engineering Commons

Authors

N. A. Krotkov, O. Torres, C. Seftor, A. J. Krueger, A. Kostinski, William I. Rose, Gregg J. Bluth, D. Schneider, and S. J. Schaefer

Comparison of TOMS and AVHRR Volcanic Ash Retrievals from the August 1992 Eruption of Mt. Spurr

N.A.Krotkov[1], O.Torres[5], C.Seftor[1], A.J.Krueger[2], A.Kostinski[2,6], W. I. Rose[3],

G J S Bluth[3], D.Schneider[1,4], and S.J.Schaefer[5]

Abstract. On August 19, 1992, the Advanced Very High Resolution Radiometer (AVHRR) onboard NOAA-12 and NASA's Total Ozone Mapping Spectrometer (TOMS) onboard the Nimbus-7 satellite simultaneously detected and mapped the ash cloud from the eruption of Mt. Spurr, Alaska. The spatial extent and geometry of the cloud derived from the two datasets are in good agreement and both AVHRR split window IR (11-12μm brightness temperature difference) and the TOMS UV Aerosol Index (0.34-0.38μm ultraviolet backscattering and absorption) methods give the same range of total cloud ash mass. Redundant methods for determination of ash masses in drifting volcanic clouds offer many advantages for potential application to the mitigation of aircraft hazards.

1. Introduction

Enormous masses of volcanic ash and gases are injected into the stratosphere and upper troposphere after major volcanic eruptions. Large (>0.5mm) ash particles fall out in minutes [*Rose et al, 1995*], but fine ash particles can remain in the atmosphere for many days. This fine volcanic ash is a hazard to modern jet aircraft because the operating temperatures of jet engines are above the solidus temperature of volcanic ash, and because ash causes abrasion of windows and airframe, and disruption of avionics. North Pacific air routes are especially vulnerable due to flight paths adjacent to a large number of Pacific Rim volcanoes [*Dean et al., 1998*]. At least 15 aircraft have been damaged since 1980 by flying through volcanic ash clouds [*USGS Fact sheet 030-97, 1997*]. A particularly dangerous incident occurred in 1989, when a KLM Boeing 747 with 231 passengers lost all engine thrust after entering an ash cloud from an eruption of Redoubt Volcano in Alaska. Engine thrust was regained only about 1000m above the Talkeetna Mountains, and $80 million worth of damages were incurred [*Casadevall, 1994*].

At large (10^2 –10^4km or more) distances from their source, drifting ash clouds are increasingly difficult to distinguish from meteorological clouds, both visually and on radar [*Rose et al., 1995*]. Satellites above the atmosphere are unique platforms for viewing volcanic clouds on a global basis and measuring their constituents and total mass [*Rose and Schneider 1996*]. Until recently, only polar AVHRR and geostationary GOES instruments [*Rose and Schneider 1996*] could be used to

determine characteristics of drifting volcanic ash clouds using the 10-12μm window [*Prata 1989; Wen and Rose 1994*]. The Total Ozone Mapping Spectrometer (TOMS) instruments were used to determine the characteristics of sulfur dioxide (SO2) clouds in the near UV spectral region [*Krueger et al, 1995*]. However, a new quantity known as the Aerosol Index (AI) has been developed for TOMS data to detect the presence in the atmosphere of ash particles [*Seftor et al., 1997*] and other types of absorbing aerosols [*Hsu et al 1996; Herman et al. 1997; Torres et al., 1998*]. In this paper, we take advantage of the fortuitous occurrence that observations by TOMS and AVHRR of the August 19, 1992 Mt. Spurr ash cloud occurred only 4 minutes apart, and thus compare virtually simultaneous ash retrievals from both ultraviolet and infrared perspectives.

2. Detection of the Mt.Spurr ash cloud

2.1 AVHRR IR data

Semitransparent ash clouds can be detected by looking at the AVHRR and GOES brightness temperature difference (BTD) between band 4 (10.3-11.5μm) and band 5(11.5-12.5μm). BTD is positive for water clouds and negative for small (radius less than ~10μm) ash particles [*Prata 1989; Wen and Rose 1994*]. The eruption of Mt.Spurr, Alaska on August 18, 1992 produced both SO_2 and ash clouds which entered the stratosphere. *Wen and Rose* [1994] examined in detail AVHRR imagery of this cloud taken 13 hours after the onset of the eruption (13:38GMT). For the purpose of comparison with TOMS data (overpass at 18:57GMT), we selected NOAA-12 AVHRR data taken at 18:53GMT, about 18 hours after the onset of the eruption and 5 hours after the image studied by *Wen and Rose* [1994]. **Figure 1(left)** shows the AVHRR BTD map (with BTD= –0.5K cut-off) (color scale) superimposed on the visible AVHRR band 1 image (gray scale). At this point, the cloud was located over the Gulf of Alaska, more than 300km SE from the Spurr Volcano, overlying low-level meteorological clouds.

2.2 TOMS AI data

The UV technique for detecting volcanic ash and other types of absorbing aerosols defines a quantity known as Aerosol Index (AI):

$$AI= -100 [\log_{10} (I_{\lambda 1}/ I_{\lambda 2})_{meas} - \log_{10} (I_{\lambda 1}/ I_{\lambda 2})_{calc}] \qquad (1)$$

where I represents the upwelling radiance at the top of the atmosphere and λ1 and λ2 are the shortest and longest available wavelengths in the 0.33-0.40μm range (where gaseous absorption is negligible). The AI is simply the difference in the logarithms of backscattered radiance at two near-UV wavelengths compared with what would be expected for a pure Rayleigh atmosphere over Lambertian surface (i.e. calculated radiances). The AI is a dimensionless quantity (one AI unit is equivalent to 2.3 %

[1]Raytheon ITSS Co, Lanham, MD 20706/ e-mail krotkov@hoss.stx.com
[2] Goddard Space Flight Center, Greenbelt, MD 20771
[3]Geological Engr. and Sciences, Michigan Technological University, Houghton, MI 49931
[4]Alaska Volcano Observatory/USGS, Anchorage, AK
[5]JCET, Univ. of MD, Baltimore County, MD
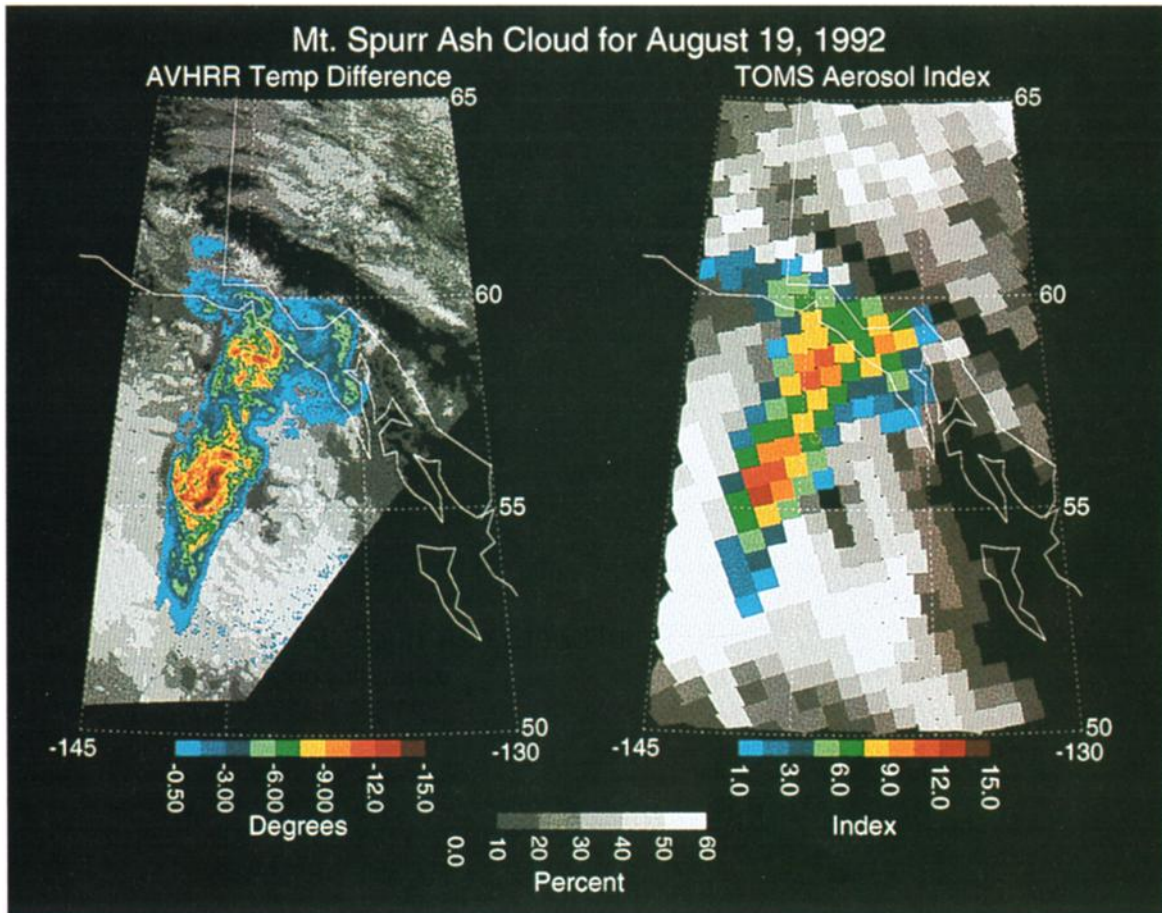[6]On sabbatical leave from Phys. Dept., Michigan Tech. University

Figure 1. Satellite maps of the August 18, 1992, Crater Peak/Spurr eruption cloud as seen by the NOAA-12 AVHRR instrument and by the NASA's Nimbus-7/TOMS instrument on August 19 at 18:57Z. The AVHRR map (left) shows the brightness temperature difference (BTD= T4 -T5 with -0.5K cutoff) as a color scale. The AVHRR band 1 is used to show the reflectivity of underlying water clouds (grey scale).The Nimbus 7 TOMS map (right) shows the Aerosol Index (λ_1=0.34μm and λ_2=0.38μm in equation (1)) as a color scale. The TOMS band at 0.38μm is used to measure the UV reflectivity of water clouds and Earth's surface (the same grey scale).

radiance change and the Nimbus 7 TOMS noise is about 0.2 units). Radiative transfer studies indicate that meteorological (water) clouds yield nearly zero AI. For absorbing aerosols they indicate that the AI is positive and increases with increasing aerosol absorption optical depth and aerosol layer height [*Torres et al., 1998*]. Tropospheric smoke and dust aerosols produce AI values up to 10, whereas ash values can be higher, mainly due to its high altitude. An advantageous AI property is the ability to detect UV-absorbing aerosols in the presence of sub-pixel clouds or over underlying clouds [*Torres et al., 1998*]. Thus, very fresh (within hours) ash clouds which contain water droplets and/or ice particles can be detected. Such clouds are difficult to distinguish from meteorological clouds in the IR data [*Wen and Rose, 1994*]. Because the reduction of aviation hazards requires mainly mapping of the spatial distribution of the ash (without regard to its microphysical properties), the AI is especially suited for that purpose.

Figure 1 (right) shows a Nimbus-7 TOMS AI map of the Mt. Spurr ash cloud (color scale) superimposed on the TOMS 0.38μm reflectivity data (gray scale). The figure indicates good agreement in the spatial extent of the ash cloud derived from TOMS and AVHRR data. Although the spatial resolution at nadir is ~1km for AVHRR data and ~50km for TOMS data, the main patterns of the ash spatial distribution revealed in the

AVHRR map can be clearly seen in the lower resolution TOMS map. We conclude that lower spatial resolution of TOMS is not a critical limitation for detection of stratospheric ash plumes significant to high-altitude aircraft operations. However, TOMS can not always detect the smaller plumes in the lower troposphere that can be detected by AVHRR or GOES.

3. Ash mass retrievals

Very little is known about how much ash a jet engine can tolerate before failure. This uncertainty could be determined by ground testing, but some information about actual ash density, particle sizes and composition would be necessary. Satellite sensors can provide this information (or at least, put some constraints on the total ash loading and microphysical properties). We start with an estimation of total mass of Mt.Spurr ash cloud. The estimation of particle sizes will be considered in a future paper.

3.1 AVHRR IR mass retrieval

A radiative transfer model [*Wen and Rose, 1994*] has been developed to convert AVHRR band 4 and 5 radiances to ash optical depth (τ) and effective particle radius (r_{eff}). The method assumes a semitransparent, single component, plane-parallel ash
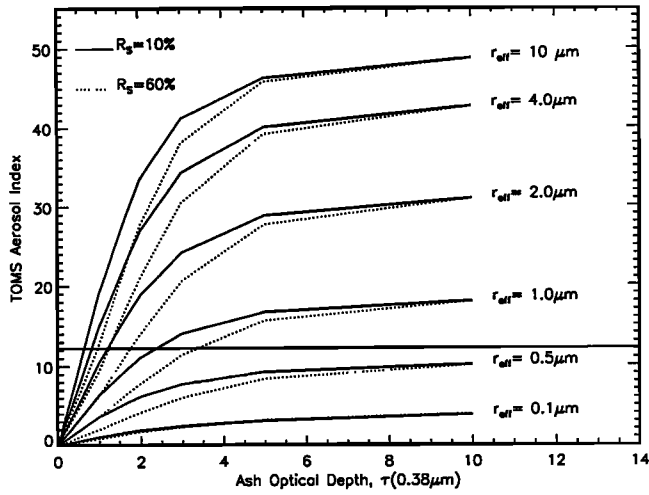
Figure 2. TOMS Aerosol Index as a function of ash optical depth (τ) at 0.38μm for different effective radius (r_{eff}) of log-normal size distribution (lnσ=0.74). Refractive index of Mt.Spurr ash ground samples (m(0.34μm)= 1.53 − 0.005i , m(0.38μm)=1.55 − 0.0052i [*Winchester 1998*]). Underlying cloud reflectivity (Rs)10% (solid lines) and 60% (dotted lines). The geometrical conditions correspond to one TOMS pixel in the center of the ash plume. The horizontal line represents a measured value of AI (~12) for this pixel.

plume, composed of homogeneous spherical ash particles with a unimodal lognormal size distribution, n(r), and known refractive index m(λ) [*Pollack et al 1973*]. *Wen and Rose* [1994] examined in detail the retrieval scheme and simplifying assumptions for the Mt. Spurr case. The inferred r_{eff} and τ data are converted to a particle mass in each pixel and in the whole cloud, M:

$$M = \sum 4/3 \rho S \, r_{eff} \, \tau \, f(r_{eff}) \qquad \text{[tons]} \qquad (2)$$

where ρ=2.6g/cm^3 is the particle mass density [*Neal et al., 1995*], S [km^2] is the pixel area, r_{eff} [μm] is effective radius and f is the dimensionless mass conversion factor = $<r^2>/<r^2 Qe>$, (averaging over particle size distribution (Qe is extinction efficiency factor),
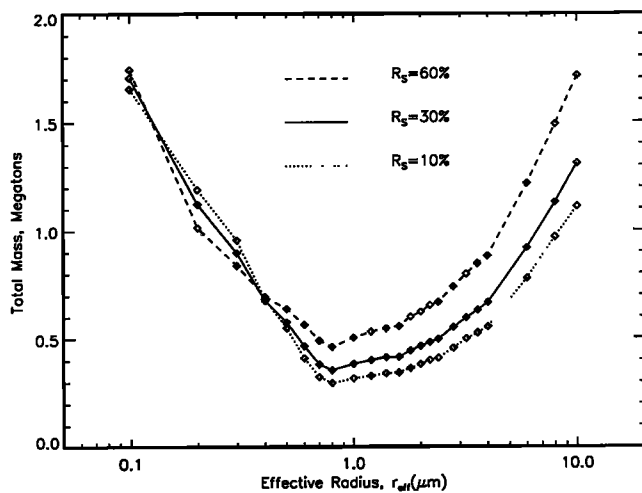

Figure 3. TOMS total ash cloud mass as a function of assumed effective radius and reflectivity of underlying clouds. Radius weighted average total mass <M>=0.7Mt, 0.8Mt and 1.1Mt for Rs= 10%, 30%, 60% respectively.

Table 1. Total mass estimation for August 19, 1992 Mt.Spurr ash cloud observed 300km away from volcano over Gulf of Alaska about 18 hours after the onset of eruption.

Instrument	Total mass, 10^6 tons			% of the total mass fallout [*Neal et al 1995*]
	Min	Max	Average	
AVHRR (IR)*	0.4	1	0.7	1% - 3%
TOMS (AI)**	0.3	1.7	0.8	1% - 6%

*According to *Wen and Rose* [1994] method: refractive index of andesite (Band 4: m(λ)=2.174 - 0.648i; Band 5: m(λ)= 1.833 - 0.131i [*Pollack et al.1973*]) and different ash size distributions.

** According to the TOMS AI fitting method (Section 3.2): measured refractive index of Mt.Spurr ash ground samples [*Winchester 1998*], log-normal size distribution with r_{eff} ranging from 0.1μm to 10μm (lnσ=0.74), and underlying cloud reflectivity, Rs, ranging from 10% to 60%. Average mass represents r_{eff} weighted average for Rs=30%. Particle mass density ρ=2.6g/cm^3 [*Neal et al, 1995*] in both methods.

f=0.5 in the geometric optics regime). Direct application of (2) to AVHRR data for the Mt.Spurr cloud produces a mass estimate of ~0.7Megatons (Mt) with column mass ranging between 1 and 10tons/km^2. The sensitivity study described in *Wen and Rose* [1994] gives the range of variation for M shown in Table 1.

3.2 TOMS AI mass retrieval

The retrieval of ash cloud mass using the spectral information contained in the TOMS AI measurements requires an inversion procedure [*Krotkov et al 1997; Torres et al 1998*]. First, the single scattering properties of the Mt.Spurr ash were computed at Nimbus-7 TOMS wavelengths (λ1=0.34μm and λ1=0.38μm) from Mie theory assuming homogeneous spherical particles and the same type of lognormal size distribution used in AVHRR retrievals. The ash refractive index, m(λ), was taken from measurements of the Mt.Spurr eruption fall-out samples [*Winchester 1998*]. The ash vertical profile was modeled as a gaussian distribution centered at 13km [*Wen and Rose 1994*], with a 1km standard deviation, embedded in a molecular atmosphere. The Gauss-Seidel polarized multiple scattering radiative transfer code [*Herman and Browing 1965*] was used to simulate the backscattered radiances at the top of the atmosphere (I$_{\lambda1}$ and I$_{\lambda1}$) and AI (equation 1) for the specific geometry of each TOMS pixel (Figure 1). An underlying Lambertian surface with reflectivity Rs was used to simulate reflection from the underlying meteorological clouds. Figure 2 shows the results of one such set of AI calculations for one TOMS pixel with maximum measured AI~12. We note that the simulated AI increases monotonically with increases in either τ or r_{eff}.

We infer τ by fitting measured (Figure 1) and simulated (Figure 2) AI values for each assumed value of Rs and r_{eff}. The total mass is calculated according to Equation (2). Figure 3 shows the total ash cloud mass M as a function of assumed r_{eff} for different Rs. We note that M(r_{eff}) has a minimum near r_{eff} ~1μm (M~0.3Mt for Rs=30%). The weighted average of M over the whole range of r_{eff} (using an area average value of Rs=30%) gives M ~0.8Mt. Changing the cutoff value of AI (Figure 1)

from1 to 0.2 increases the number of ash contaminated pixels, but increased M by less than 5%.

Comparisons of AVHRR and TOMS mass retrievals are given in Table 1. We note that the TOMS mass range (0.3-1.7Mt) agrees with AVHRR mass retrievals (0.4 - 1Mt). A vast majority of the pyroclastic materials produced in the eruption of Spurr and other volcanoes was larger than 1mm in diameter and fell out of the atmosphere in less than 30 minutes [*Rose et al, 1995*]. After 18 hours of transport only particles that are smaller than about 25μm in radius are present and these particles represent a small fraction of the total mass. The TOMS and AVHRR masses estimated for the 18 hour old drifting volcanic cloud erupted from Mt. Spurr on 19 August 1992 represent 1-6% of the total mass of the ash produced [36,400 kT; *Neal et al 1995*]. These results are consistent with heavy fallout of coarse ash (representing the bulk of the mass) near the volcano (*R. G. McGimsey, personal communication*), and a vulcanian fragmentation process that perhaps produces proportionally smaller amounts of fine ash than plinian or phreatoplinian eruptions [*Murrow et al 1980; Neal et al 1995*].

4. Conclusions

Both TOMS and AVHRR can detect drifting volcanic ash clouds, which pose a danger to jet aircraft. The TOMS AI reflectance technique requires solar illumination but can detect very fresh (within minutes to hours) ash clouds, which appear opaque in the AVHRR IR data. In this first direct intercomparison between the AVHRR two band temperature difference and the TOMS AI method of computing mass, we find the same range of total cloud ash mass using available data on the ash index of refraction and consistent assumptions about ash cloud composition.

The location of UV (TOMS) and IR (AVHRR) instruments on polar platforms with different local equator crossing times provides only rare coincident measurements of drifting volcanic ash clouds. This situation is inadequate for real time ash monitoring. We suggest the combination of UV and IR channels into one instrument suite on a geostationary platform could provide both frequent observations with redundant capability that would be effective for learning how to improve measurements and reduce aircraft hazards.

References

Casedevall, T.J., The 1989-1990 eruption of Redoubt Volcano, Alaska: Impacts on aircraft operations, *J. of Volcanology and Geothermal Research*, 62, 301-316, 1994.

Dean, K., M.Servilla, A.Roach, B.Foster, and K.Engle, Satellite Monitoring of Remote Volcanoes Improves study efforts in Alaska, EOS, Transactions, 79, 35, pp.413,423, 1998

Herman, B.M., and S.R. Browing, A numerical solution to the equation of radiative transfer, *J.Atmos.Sci.*, 22, 559-566, 1965

Herman, J.R., P.K.Bhartia, O.Torres, N.C.Hsu, C.J.Seftor, and E.Celarier, Global distribution of UV-absorbing aerosols from Nimbus-7/TOMS data, *J. Geophys.Res.*, 102, 16911-16922, 1997

Hsu, N.C.,J.R.Herman, P.K.Bhartia, C.J.Seftor, O.Torres, A.M.Thompson, J.F.Gleason, T.F.Eck, and B.N.Holben, Detection of biomass burning smoke from TOMS instruments, *Geophys. Res. Lett.*,23, 745-748, 1996

Krotkov N.A., A.J.Krueger, P.K.Bhartia, Ultraviolet optical model of volcanic clouds for remote sensing of ash and sulfur dioxide, *J. Geophys.Res*, 102, 21891-21904,1997

Krueger A.J., L.S.Walter, P.K.Bhartia, C.C.Schnetzler, N.A.Krotkov, I.Sprod, and G.J.S.Bluth, Volcanic sulfur dioxide measurements from the Total ozone Mapping Spectrometer (TOMS) instruments, *J. Geophys.Res*, 100,14057-14076, 1995

Murrow, P.J., W.I.Rose and S.Self, Determination of the total grain size distribution in a vulcanian eruption column and its implications to stratospheric aerosol perturbation, *Geophys. Res. Lett.*, 7, 893-896, 1980

Neal C.A., et al., Tephra-fall deposits from the 1992 eruptions of Crater Peak, Mount Spur volcano, Alaska: A preliminary report on distribution, stratigraphy, and composition, *U.S. Geol. Surv. Bull*, 2139:65-79, 1995

Pollack, J.B., O. Toon, and B.N.Khare, Optical properties of some terrestrial rocks and glasses, ICARUS, 19, 372-389, 1973

Prata, A.J., Observations of volcanic ash clouds in the 10-12μm window using AVHRR/2 data, *Int. Journ. Rem. Sens.*10, 751-776, 1989

Rose, W.I., A.B.Kostinski and L.Kelley, Real time C band radar observations of 1992 eruption clouds from Crater Peak/Spurr volcano, Alaska, *U.S.Geol.Surv. Bull.* 2139,19-26, 1995

Rose, W. I., and D. J. Schneider, Satellite images offer aircraft protection from volcanic ash clouds, *EOS*, 77, 529-532, 1996

Seftor, C.J., N.C.Hsu, J.R.Herman, P.K.Bhartia, O.Torres, W.I.Rose, D.J. Shneider, and N.Krotkov, Detection of volcanic ash clouds from Nimbus-7/Total Ozone Mapping Spectrometer, *J. Geophys. Res.*, 102, 16749-16759, 1997

Torres, O., P.K.Bhartia, J.R.Herman, Z.Ahmad, and J.Gleason, Derivation of aerosol properties from satellite measurements of backscattered ultraviolet radiation: Theoretical basis, *J. Geophys. Res.*, 103, 17099-17110, 1998

Wen, S. and W.I. Rose, Retrieval of particle sizes and masses in volcanic clouds using AVHRR bands 4 and 5, JGR, 99:5421-5431, 1994

Winchester L.W., Determination of the Complex refractive index of samples of volcanic ash, NASA contract report, No. S-01394-G, 1998 (Available from the corresponding author).